

An NQR study of thermally activated molecular motion in 5-Choloro-3-Pyridinol

**Disusun oleh:
Philips Nicolaś Gunawidjaja**



**FAKULTAS MATEMATIKA DAN ILMU PENGETAHUAN ALAM
UNIVERSITAS KATOLIK PARAHYANGAN
BANDUNG
2007**

Abstract

A study of the temperature dependence of ^{35}Cl NQR frequency and spin-lattice relaxation time in 5-chloro-3-pyridinol is reported. The project investigated the existence of crystalline phases and the behaviour of T_1 at varying temperatures, which allowed the determination of the activation energy of the compound. The data indicates the existence of a single crystalline phase with two resonance lines. Value of activation energy of the motions of the compound was calculated to be $11.9 \pm 1.3 \text{ kJ mol}^{-1}$.

Content

1	Introduction	1
2	Background Theory	1
	2.1 Theory of Nuclear Quadrupole Resonance.....	1
	2.1.2 Excitation and Detection of Resonances.....	3
	2.1.3 Measurement of Spin-Lattice Relaxation Times.....	4
	2.2 Theory of Spin Lattice Relaxation.....	6
3	Experimental Details	7
4	Results	8
5	Analysis and Discussion	11
	5.1 Spin-Lattice Relaxation Time Data.....	11
	5.2 NQR Frequency and line width measurement.....	11
	5.3 Problems encountered during the experiment.....	11
	5.4 Suggestion for Future Improvement.....	12
6	Conclusion	12
	Acknowledgement.....	12
	References.....	12

1. Introduction

Nuclear Quadrupolar Resonance (NQR) is a widely used technique for studying thermally activated molecular motion in solids. As is referred by S.C. Perez in his paper, the nuclei being observed can in principle be located either inside or outside the moving molecular fragments. In the latter case it is necessary, in order to detect the molecular motions, that the electric interactions between the moving fragments and the resonant nuclei produces a sufficient modulation of the spin-lattice coupling [1, 2].

The present study involves chlorine NQR measurements in 5-chloro-3-pyridinol. Figure 1 shows a schematic illustration of the constituent molecules. Unfortunately, the crystal structure for this compound is not known.

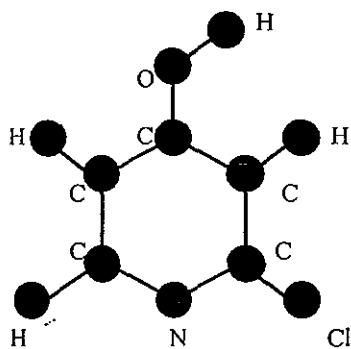


Figure 1. The molecular structure of 5-chloro-3-pyridinol (C_5H_4NOCl)

The project investigated the existence of crystalline phases and the behaviour of the spin-lattice relaxation time, T_1 , at varying temperature, which allowed the determination of the activation energy of the compound. Measurements of the resonance frequency, ν_Q , line width $\Delta\nu$ and spin-lattice relaxation time, T_1 , are reported as a function of temperatures for the ^{35}Cl nuclei of 5-chloro-3-pyridinol.

Section 2 contains a brief explanation of the background theory of NQR and the relationship between relaxation times and its motion. A brief overview of experimental procedures is given in section 3. The results are presented in section 4. Current analysis and discussion of the data are given in section 5, with details to each result, problems encountered, and suggestions for future improvements presented in subsections. Brief conclusions are given in section 6.

2. Background Theory

A basic knowledge of NQR is essential to understand the science behind this project. It is important to understand both how the method works and how results are interpreted using NQR as an analysing tool. This section of work will explain some of the most important theories of NQR related to the project.

2.1 Theory of Nuclear Quadrupole Resonance

Originated in 1950s, Nuclear Quadrupole Resonance is one of the special branches of radio-frequency spectroscopy physics that is being used increasingly as an analytical tool for solid state studies and structural chemistry. It is an extremely useful method of observing nuclei with spins $>1/2$. Comprehensive review to explain the features of the quadrupole spectra and to show how they are interpreted in terms of the electron distributions that produce the necessary electric field gradients at nuclei can be found in a book written by T.P. Das and E.L. Hahn (1958) [3].

The fundamental analysis and description of nuclear electric quadrupole interactions have been given in a book¹ written by Cohen and Reif. Quantum-mechanical Hamiltonian describing the interaction of the nuclear quadrupole moment with the surrounding charge distribution, and treating the case where the

¹ M. H. Cohen and F. Reif, Nuclear quadrupole effects in nuclear magnetic resonance. *Solid State Phys.* 5, 321 (1957).

electric quadrupole interaction is a small perturbation upon the interaction between the magnetic dipole moment of the nucleus and a large applied magnetic field, was described.

This section of work, will underline some of the most important theories, extracted from the above article, which form the most basic block of NQR theory.

In the conventional radio-frequency spectroscopy experiment, a strong steady magnetic field is present, perpendicular to which a radio-frequency magnetic field is applied and the free induction and echo signals following the application of the radio-frequency field in short pulses, is studied. This technique is widely known as Nuclear Magnetic Resonance. In the case of pure quadrupole resonance, the nuclear electric quadrupole interaction forms the basis of a separate kind of radio-frequency spectroscopy based on the orientational quantisation of the nuclei along the internal principal electric-field gradient direction. This technique, called the Nuclear Quadrupole Resonance (NQR), requires no external magnetic field, but can be otherwise applied to samples using NMR technology. In this case, one can think of radio-frequency spectroscopy experiments where the electric field gradient, which is generated by asymmetric electron distributions in molecules or lattice sites, inside the crystal takes the place of the steady magnetic field.

The interaction between the quadrupole moment of nuclei and electric field gradient is described by the nuclear electric quadrupole tensor (either in zero or non-zero magnetic field). Since the experiment only concern with zero field interaction, only NQR in zero field will be consider.

The Hamiltonian characterising this interaction in zero field is given by the equation:

$$H_Q = \mathbf{Q} \cdot \nabla E = \sum Q_2^m (\nabla E)_2^{-m} \quad \text{---(1)}$$

As a result of this interaction, the nuclei possesses an energy diagram shown below:

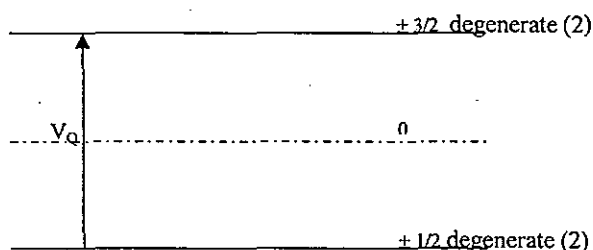


Figure 2. The energy levels, in zero magnetic field, for $I = 3/2$

The difference between one energy level and the next gave the nuclear quadrupolar resonance frequency, which can be described by the equation:

$$V_Q = e^2 q Q (1 + \eta^2/3) / 2h \quad \text{---(2)}$$

Note that V_Q does not depend on orientational parameters and that other interactions can be ignored.

2.1.2 Excitation and Detection of Resonances

In NQR spectroscopy, the magnetic component of an applied radio-frequency field stimulates transitions between the nuclear quadrupole energy levels. One common technique that is used to achieve this condition is the polychromatic excitation of the entire spectrum by short pulses at a carrier frequency ν_0 and fixed magnetic field strength.

To explain pulse NQR experiments, it is useful to appeal to the classical predictions that the interaction of the nuclear magnetic moments with the magnetic field forces the nuclei to precess around the field direction with the Larmor frequency:

$$\nu_p = (2\pi)^{-1} \gamma B_{loc} \quad \text{---(3)}$$

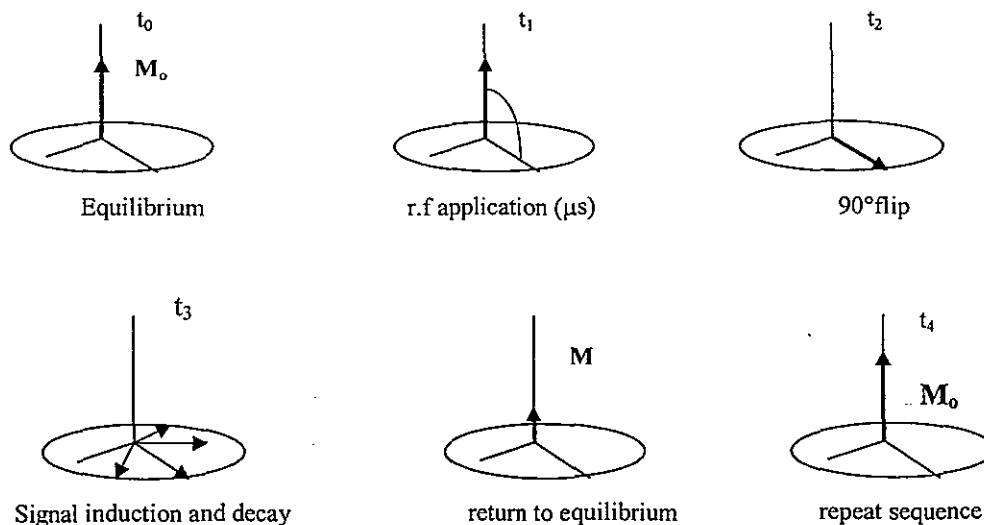
The macroscopic magnetisation, which forms at spin-lattice equilibrium as a result of the Boltzmann distribution, is the target of the pulsed NQR experiment. To measure the NQR spectrum of the sample, this magnetisation is converted to a nuclear induction signal. The principle is illustrated with vector diagram depicted in the "rotating frame", i.e. a co-ordinate system that rotates with the carrier frequency ν_0 about the magnetic field axis (as shown in figure 3). A short (1-10 μ s length), intense (100-1000 Watt power) radio-frequency pulse is applied that tips the magnetisation into the plane perpendicular to the electric field direction ("90° pulse"). The pulse must be applied at a carrier frequency ν_0 in the vicinity of ν_p . Precise resonance is, however, not required, since pulsed excitation is in itself polychromatic. Since samples with multiples sites have a range of values of ν_p , it is important, however, that the Fourier Spectrum includes the entire range of such precession frequencies. In polycrystalline solids, the required range is typically 100-299 kHz, which is easily covered by short pulses.

In certain cases, site distribution effects generate much wider ranges of resonance frequencies. Such broad lines can be mapped out by spin echo spectroscopy under systematic variation of the carrier frequency ν_0 .

Following the 90° flip by the radio-frequency excitation pulse, the magnetisation precesses with the ν_p components of the nuclei present and induces an a.c. voltage in the detector coil of the NQR probe. This voltage signals decays in time because the magnetisation vectors lose their phase coherence due to their differences in ν_p as well as due to spin-spin interactions. The "free induction decay" is amplified, and is mixed in the receiver section of the spectrometer with the carrier frequency ν_0 . The resulting signal then oscillates at the difference frequency $\nu_{\text{offset}} = |\nu_p - \nu_0|$ and is typically in the audio frequency range (0-200 kHz). If chemically distinct sites are present, this signal is a decaying interferogram ("beating pattern") of several different frequency components. Fourier Transformation of this digitised and stored interferogram then yields the various ν_{offset} (and hence the ν_p) components.

Since the acquired signals are quite weak, signal averaging by repetitive pulsing is usually necessary. A 90° pulse creates a state of equally populated nuclear spin levels. Hence no z-magnetisation is present immediately after the pulse, and one must allow for sufficient time for the spin system to relax to its equilibrium state. For quantitative application, the repetition must exceed 5 times the longest spin-lattice relaxation time present in the sample.

(a)



(b)

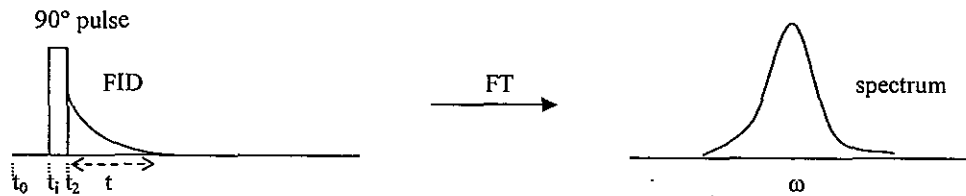


Figure 3. (a) Detection of NQR signals by pulsed spectroscopy, shown in the rotating co-ordinate system associated with the oscillating electric field component at the applied radio-frequency ω_0 at various stages (t_0 - t_4) of the experiment t_0 - spin system with magnetisation direction tips the magnetisation, t_2 -the system after a 90° pulse resulting in transverse magnetisation M_t , t_3 -off resonance precession and free induction decay in the signal acquisition period following the pulse, t_4 -return to spin equilibrium due to spin lattice relaxation. (b) Timing diagram of the experiment followed by Fourier Transform. (H. Eckert, (1992). 'Structural characterisation of noncrystalline solids and glasses', *Progress in NMR spectroscopy*, 24, pp. 179).

When one works with a low- γ nuclei, however, the ringing in the probe affects the recovery of the receiver and results in a large spurious free induction decay signal, which often completely obliterates the NQR signal. To overcome this problem, the spin-echo technique is used. The pulse sequence used is basically a Hahn echo:

$$(\theta_1)\phi_1-\tau-(\theta_2)\phi_2-\tau_2-(AQ)\phi_3 \quad \text{---(4)}$$

The intervals τ_1 and τ_2 are the spacings between the two pulses and the time for echo formation after the second pulse respectively, and were usually varied between 30 and 70 μs . The phase cycling was designed to cause destructive interference of the spurious free induction decay (FID). The coaddition of the spin-echo signals along x , y , x , or \bar{y} was found to be particularly good sequence for removal of real baseline artifacts from the spin-echo data. The pulse widths used are θ_1 and θ_2 ; θ_1 was typically a 45° or 90° (solid) pulse, and θ_2 was twice the length of θ_1 . The shorter pulse widths are desirable when the overall spectral breadth is very large. Figure 4 shows the spin-echo sequence:

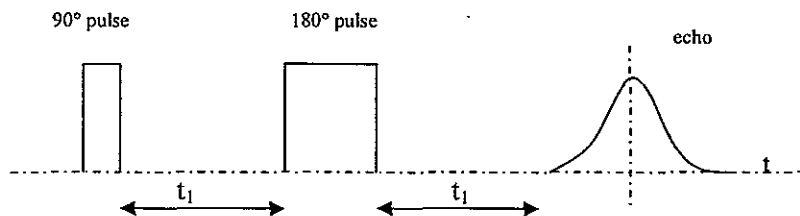


Figure 4. Detection of NQR signal using spin-echo sequence.

2.1.3 Measurement of Spin-Lattice Relaxation Times

There are two methods to measure the spin-lattice relaxation time, T_1 . These are shown in figure 5a and b respectively. The inversion recovery method $180^\circ-\tau-90^\circ$ measures the re-establishment of longitudinal magnetisation at the time t_1 after the magnetisation has been inverted by a 180° pulse; T_1 is determined from a series of measurements with different values of t_1 using, using the relationship

$$I(t_1) = I(0) (1-2\exp^{-t_1/T_1}) \quad \text{---(5)}$$

It is, however, often difficult to provide uniform excitation over the entire spectral region by a 180° pulse. Alternatively, the saturation recovery method $(90^\circ)_n-t_1-90^\circ$ can be used. In this case, the re-establishment of the longitudinal relaxation after saturation of the spin system by the 90° pulse train is given by

$$I(t_1) = I(0) (1-\exp^{-t_1/T_1}) \quad \text{---(6)}$$

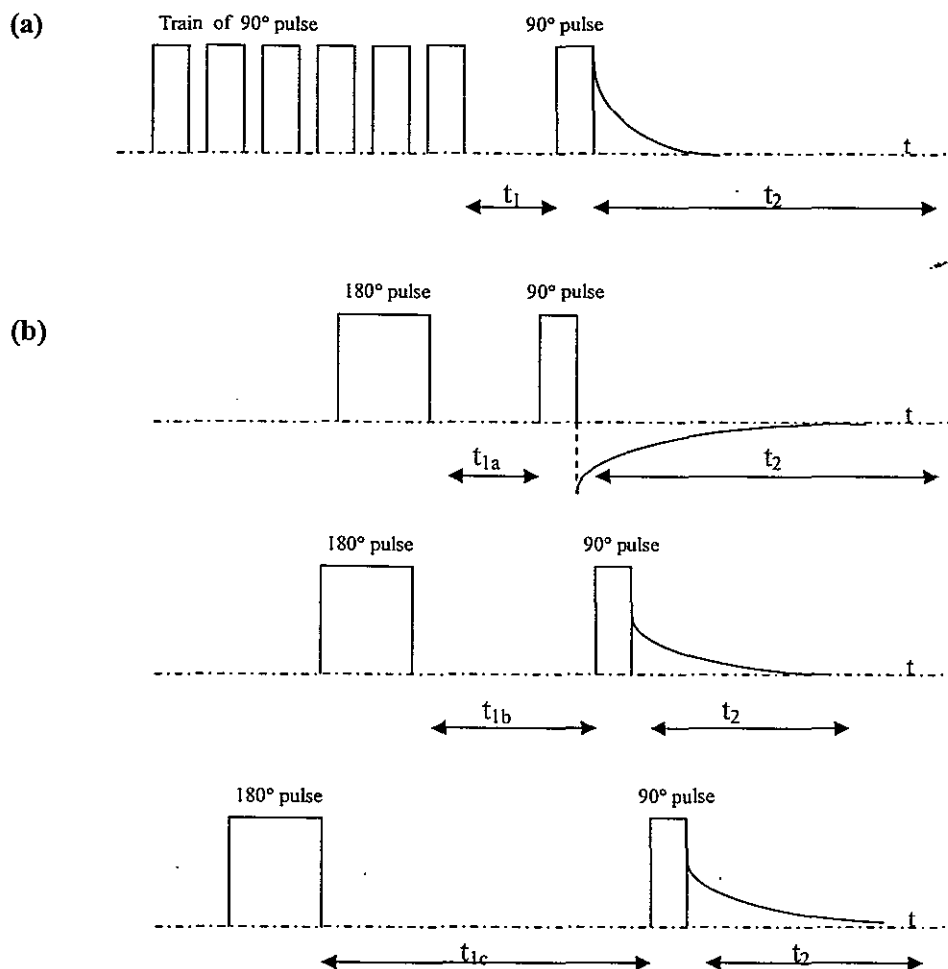


Figure 5. Measurement of the spin-lattice relaxation time by (a) the saturation recovery $(90^\circ)_n-t_1-90^\circ$ method and (b) the inversion recovery $(180^\circ-t-90^\circ)$ method. For the latter, the signal build-up is shown for three evolution times t_{1a-c} elapsing between the preparation pulses and the final 90° detection pulse. (H. Eckert, (1992). 'Structural characterisation of noncrystalline solids and glasses', *Progress in NMR spectroscopy*, 24, pp. 180).

2.2 Theory of spin lattice relaxation

Comprehensive review to explain the theory of spin lattice relaxation can be found in the article written by H. Eckert (1992) [4]. This section of work will underline the basic principle of spin lattice relaxation extracted from the above article.

Nuclear electric quadrupole interaction is based on the orientational quantisation of the nuclei along the internal principal electric field gradient direction. Due to the energy splitting, the spin-state population distribution follows a familiar Boltzmann distribution at thermal equilibrium, resulting in a macroscopic magnetisation.

The change in the population distribution following the radio-frequency excitation changes the energy of the spin system; it hence involves energy transfer between the spin system and its surroundings (the "lattice"). The attainment of thermal equilibrium can be described by first-order kinetics and characterised by the time constant T_1 , which is known as the spin-lattice relaxation time. Microscopically, relaxation is caused by fluctuating magnetic fields from unpaired electrons, conduction electrons, or modulated magnetic dipole-dipole interactions. For nuclei with spin $> \frac{1}{2}$, fluctuating electric field gradients are an efficient source of relaxation. Whichever mechanism dominates, relaxation can be effected either directly or through spin-diffusion via magnetic dipole-dipole couplings.

Dynamical processes such as atomic or molecular motion result in fluctuating dipolar or quadrupolar interactions, and hence facilitate spin lattice relaxation. The relaxation efficiency is determined by the

overlap between the frequency spectrum of the motional process and the resonance frequency. This means that there must be a good match between the energy released from the spin system upon its return to the Boltzmann state and the energy quanta that the lattice is apt to accommodate. This match is described by the spectral density $J(\omega\tau_c)$. Since $J(\omega\tau_c)$ is the Fourier Transform of the correlation function describing the motion, its functional form depends on the mechanism of motion. For an exponential correlation function:

$$J(\omega\tau_c) = \tau_c (1 + \omega^2\tau_c^2)^{-1} \quad \text{---(7)}$$

A plot of $J(\omega\tau_c)$ as a function of ω is seen in Figure 2, for the three regimes $\omega_0\tau_c \ll 0$, $\omega_0\tau_c \approx 1$, $\omega_0\tau_c \gg 1$.

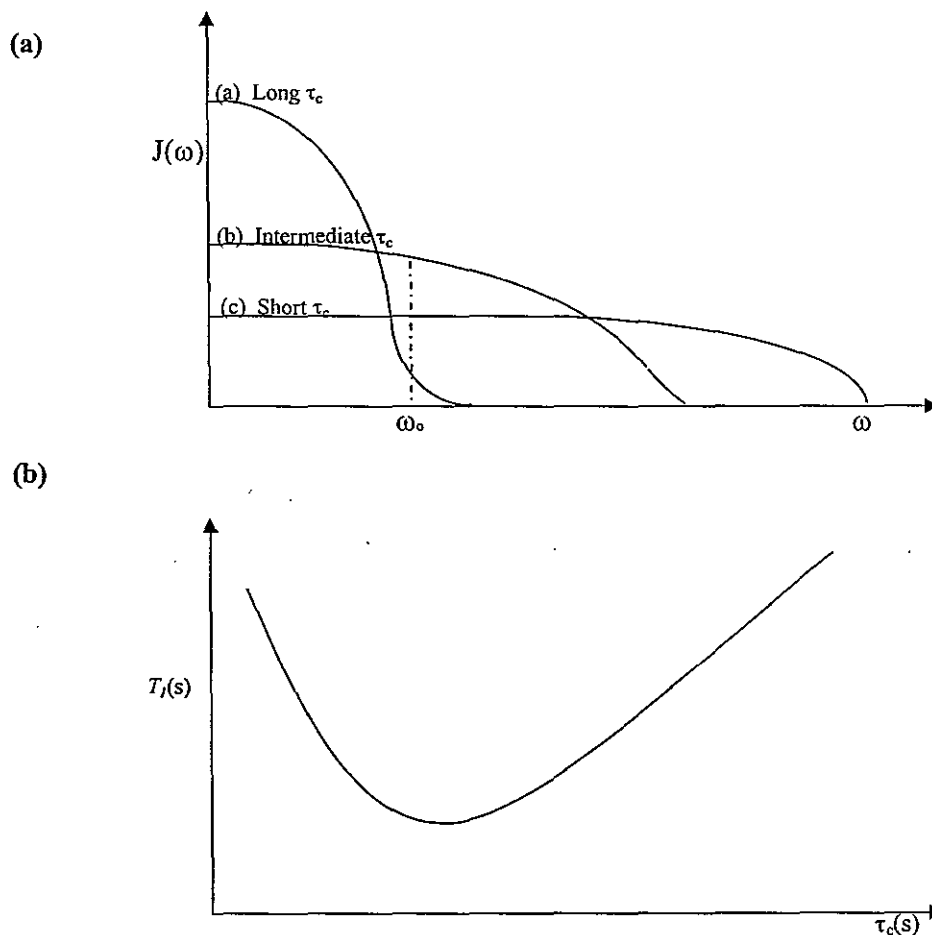


Figure 6. Top: Frequency dependence of the spectral density function in the extreme narrowing limit ($\omega_0\tau_c \ll 1$), the slow motion limit ($\omega_0\tau_c \gg 1$) and the intermediate region $\omega_0\tau_c \approx 1$. Bottom: Typical dependence of the spin lattice relaxation time T_1 on frequency and correlation time τ_c . (H. Eckert, (1992). 'Structural characterisation of noncrystalline solids and glasses', *Progress in NMR spectroscopy*, 24, pp. 177).

Considering relaxation by stochastic motion, Bloembergen, Purcell, and Pounds (BPP) derived the following general expression for the spin-lattice relaxation rate $1/T_1$:

$$1/T_1 = C(\tau_c/(1 + \omega_0^2\tau_c^2) + 4\tau_c/(1 + 4\omega_0^2\tau_c^2)) \quad \text{---(8)}$$

The constant C depends on which fluctuating interaction (dipolar, quadrupolar, or chemical shift) governs the relaxation process. C can be determined numerically from the Hamiltonian parameters governing the static lineshape in the rigid lattice limit.

In principle, equation 8 allows detailed insights into dynamical processes via temperature- and frequency-dependent measurement of T_1 . Application generally assume an Arrhenius-type relationship between τ_c and temperature:

$$\tau_c = \tau_{co} \exp(E_A/RT) \quad \text{---(9)}$$

Where τ_{co} is 1/ the attempts frequency and E_A is the activation energy of the motional, process dominating the relaxation. For the high temperature side ($\omega_0\tau_c \ll 1$), equation 8 simplifies to:

$$\ln T_1^{-1} = \ln(5C\tau_{co}) + E_A/RT \quad \text{---(10)}$$

In the limit of low temperature ($\omega_0\tau_c \gg 1$), one obtains

$$\ln T_1^{-1} = \ln(8C\omega_0^{-2}\tau_{co}^{-1}) - E_A/RT \quad \text{---(11)}$$

Thus symmetrical curves of $\ln T_1^{-1}$ against inverse temperature are expected, with a maximum at the temperature for which $\omega_0\tau_c = 1$ (Other investigators plot instead $\ln T_1$ against inverse temperature, yielding a minimum when relaxation is most effective, see figure 6 bottom). In either case, E_A is accessible from both the high- and the low-temperature sides of such plots.

Experimental studies usually comprise detailed temperature- and frequency dependent measurements of T_1 , from which the activation energy E_A and the pre-exponential factor τ_{co} can be extracted by computer fitting. In glasses, the large majority of NMR relaxation measurements have concentrated on characterising ionic diffusion processes. The discussions of the characteristic deviations from BPP behaviour are detected, suggesting either distributed correlation times or non-exponential correlation functions.

3. Experimental details

The specimens used for the experiments were obtained from Aldrich Chemical Co. and used without further purification. Five compounds were investigated during the experiment. They were NaClO_3 (#24, 414-7), 6-chloro-2-pyridinol (98%) (#13, 678-6), 2-chloro-3-pyridinol (98%) (#11, 620-3), 5-chloro-3-pyridinol (99%) (#21, 800-6), and 5-chloro-2,3-pyridinediol (95%) (#13, 107-5). Of the five samples investigated, however, only two compounds could be analysed, NaClO_3 and 5-chloro-3-pyridinol. The rest of the samples show no signals when being measured.

The NaClO_3 was used as an introductory compound for the project and, since only 5-chloro-3-pyridinol compound produced measurable experimental data, the present study involves chlorine NQR measurements in 5-chloro-3-pyridinol.

The sample container was a cylinder of length 40 mm and diameter 10 mm; the amount of sample used was approximately 5 g. The measurements were performed on a BRUKER MSL 300 system (see figure 7). The temperature was controlled to within ± 0.5 K using a Bruker variable temperature unit. Copper-constantan thermocouples were used to measure the temperature.

In the measurement of NaClO_3 , the spin-lattice relaxation time was determined from a single 90° pulse of length 10 μs , and a dead time following the pulse of 15 μs . The NQR frequency was measured from the spectrum obtained from the Fourier Transform (FT) of the free induction decay which came from saturated 90° pulse² [5] of length 10 μs and separated in steps of 1 ms.

In the measurement of 5-chloro-3-pyridinol, the spin-lattice relaxation time was determined from inversion-recovery pulse³ [5] sequence data and the NQR frequency was measured from the spectrum obtained from the FT of an echo delay after a $\pi/2$ and π echo pulses. The $\pi/2$ pulse is of length 9 μs and the following π pulse is of length 18 μs . The temperature range covered was between 296 K and 361 K.

² R.K. Harris, Nuclear Magnetic Resonance Spectroscopy, Pitman, London, 1983, pp. 72-74

³ R.K. Harris, Nuclear Magnetic Resonance Spectroscopy, Pitman, London, 1983, pp. 81-82

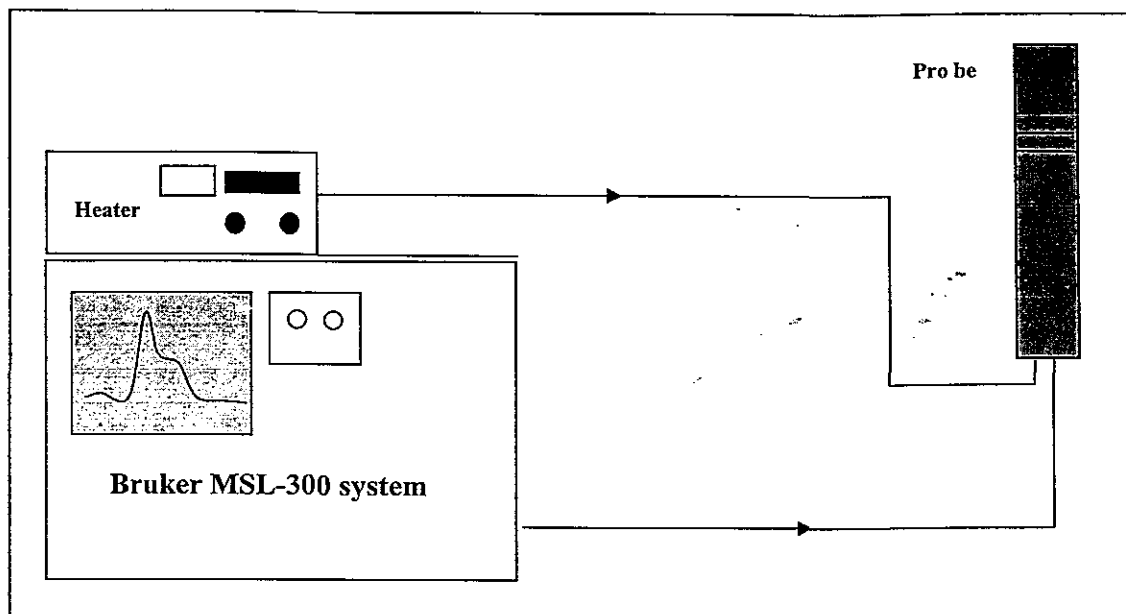


Figure 7. The equipment system used to investigate 5-chloro-3-pyridinol compound.

4. Results

The NQR signal of NaClO_3 was detected at a frequency of 29.92 MHz at 296 K and the spin-lattice relaxation time, T_1 , was 0.63 seconds. The measured values were consistent with the study conducted by Bloom and Norberg (1954) [6, 7].

A sample result of an NQR spectrum of 5-chloro-3-pyridinol is as shown in figure 8.

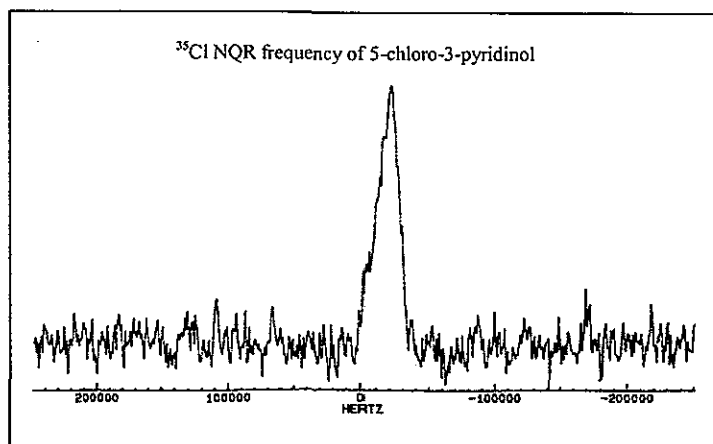


Figure 8. A sample result of an NQR spectrum of 5-chloro-3-pyridinol

The NQR signal of 5-chloro-3-pyridinol was detected at a frequency of 35.14 MHz at 306 K, and a decrease of $\pm .02 \text{ MHz}$ was noted for each increase of $\pm 5 \text{ K}$. The measured values were as expected as similar compounds of the same group, published in the article by C.J Turner (1975) [8], give similar values. A single crystalline phase with two resonance lines was observed in the measurement of 5-chloro-3-pyridinol, which indicates two chemically inequivalent positions for the chlorine nuclei in the unit cell. The spectrums obtained are illustrated in figure 9. It can be seen that the resonance frequency decreases progressively as the temperature is increased.

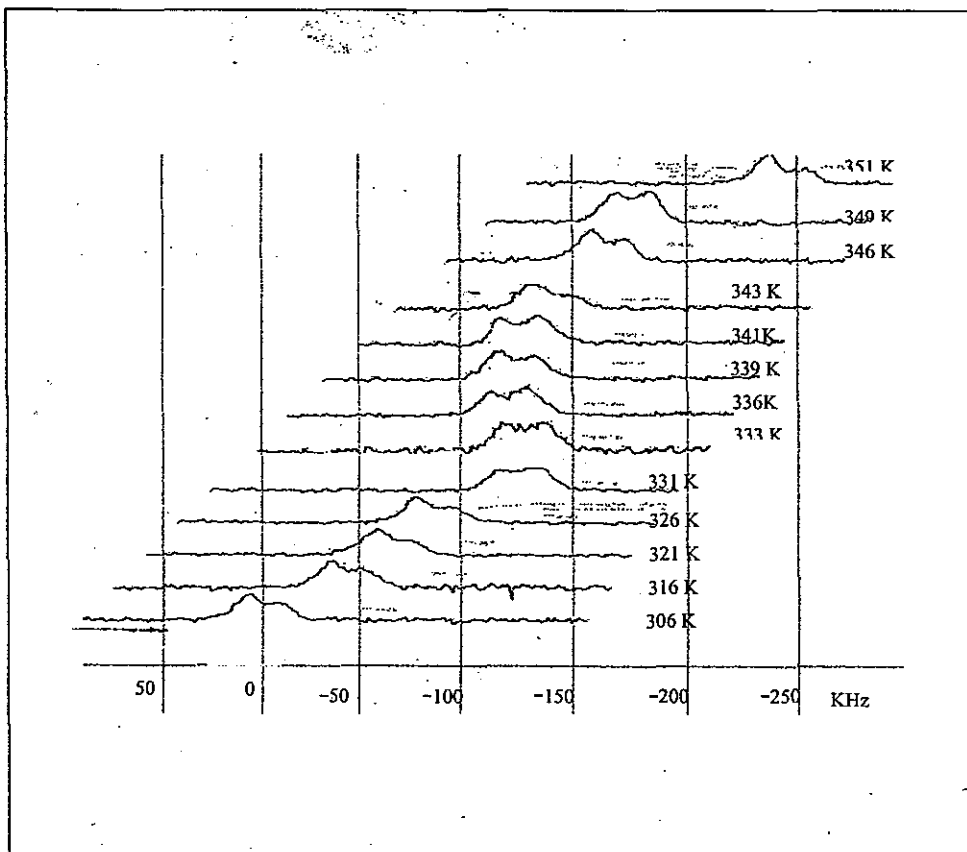


Figure 9. ^{35}Cl NQR spectra of 5-chloro-3-pyridinol heated at temperatures range of 306-351K.

The graphic representation of the temperature dependence of the peaks in the resonance frequency of 5-chloro-3-pyridinol is shown in figure 10. It can be seen that the decrease of the peaks in the resonance frequency, to within experimental error, is linear. Figure 11 shows the graphic representation of the temperature dependence of the spin-lattice relaxation times of 5-chloro-3-pyridinol. It is shown from the graph that the T_1 data fits the line nicely. The data from figure 11 also permits the determination of the activation energy for the motions of the compound.

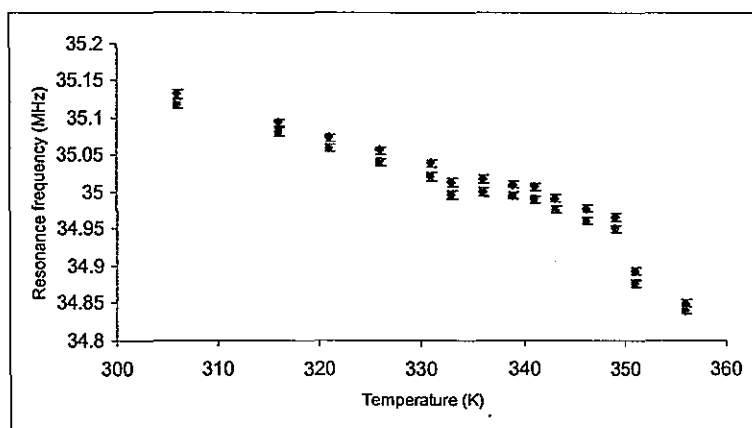


Figure 10. The temperature dependence of the ^{35}Cl NQR frequency in 5-chloro-3-pyridinol.

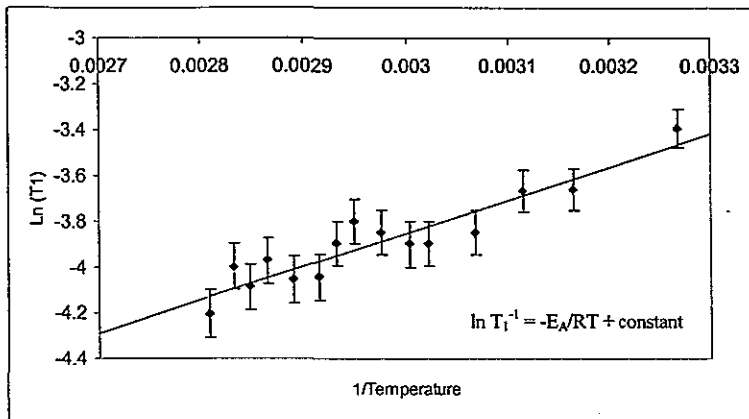


Figure 11. The temperature dependence of the ^{35}Cl T_1 values in 5-chloro-3-pyridinol.

Figure 12 and 13 show the temperature dependence of 'Differential Scanning Calorimetry' and 'Thermogravimetric Analysis', which show the behaviour of compound as the temperature is increased. It is shown in figure 12 that, between 20°C and 120°C, the energy taken in by the compound is constant. This is an indication that the compound is not changing phase, which is expected. In addition, it is shown in figure 13 that within temperature experimental range, the compound does not experience a change in mass, i.e. it does not decompose. These two results are consistent with the results obtained from the temperature dependence of spin-lattice relaxation time, resonance frequency, as well as the line widths.

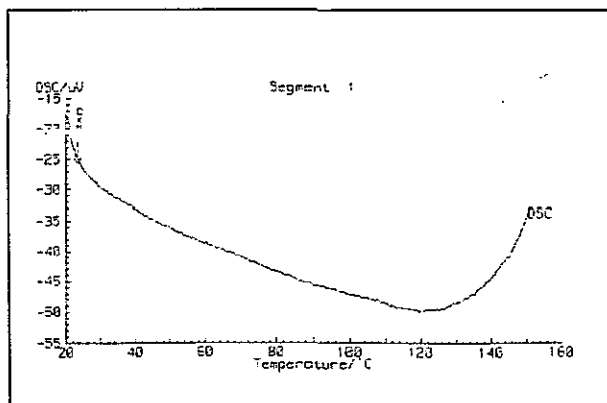


Figure 12. The Differential Scanning Calorimetry in 5-chloro-3-pyridinol

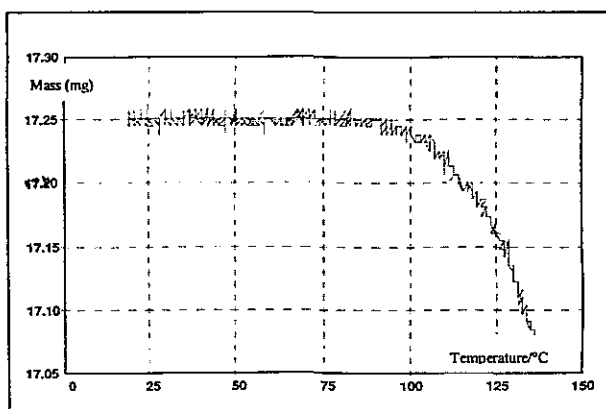


Figure 13. The Thermogravimetric analysis in 5-chloro-3-pyridinol.

5. Analysis and discussions

5.1. Spin-lattice relaxation time data

The spin-lattice relaxation times data was fitted using SIMFIT inversion recovery T_1 data fitting. The equation used to find T_1 is:

$$I = I_0 * [1 - 2 * a * \exp(-\tau/T_1)] \quad \text{---(12)}$$

It is unfortunate that, from the results obtained, it was not possible to deduce the type of vibration causing the relaxation. It was suggested (T.P. Das and E.L. Hahn (1958) [3]) that the relaxation was mainly due to libration of the benzene ring in 5-chloro-3-pyridinol. By plotting a graph of $\ln T_1$ against $1/T$ as in figure 11, and using the equation:

$$\ln T_1^{-1} = \ln(5C\tau_{co}) + E_A/RT \quad \text{---(13)}$$

It is possible to calculate the activation energy, which might be due to the libration of the compound. The activation energy obtained for this motion is calculated to be $\approx 11.9 \pm 1.3 \text{ kJ mol}^{-1}$. The measured value was as expected as similar compounds, studied by S.C. Perez (1993) [1, 2], are of the same magnitude as the measured value of the activation energy.

Another factor that can be accounted for in terms of the independent relaxation mechanism for the spin-lattice relaxation time of the ^{35}Cl nuclei observed in 5-chloro-3-pyridinol, is the modulation of the OH group adjacent to the molecule. X-ray structure is needed to confirm this modulation. It is unfortunate that it is not possible to prove the modulation effect from the data obtained in the experiment.

5.2. NQR frequency and line width measurements

No broadening in the line width related to the reorientation of the ^{35}Cl in 5-chloro-3-pyridinol was observed, which indicates that the compound is vibrating in the lattice rigid limit as it is heated. This is expected since there is no evidence of phase change in the entire experiment.

Measurement of the temperature dependence of the resonance frequency, ν , indicates the existence of a single crystalline phase with two resonance lines which suggests the presence of two chemically inequivalent positions for the chlorine nuclei in the unit cell. The inequivalent positions for the chlorine nuclei in the unit cell might be due to the sample not being fully crystallised or the presence of impurities in the compound. Unfortunately, there was insufficient time to re-crystallise the substance and investigate the results.

No evidence of phase change was observed in the experiment as the decrease in the resonance frequency is, within experimental error, linear (decrement of $\approx 20 \text{ kHz}$ for each increase of 5 K). This result is consistent with the data obtained from the temperature dependence of 'Differential Scanning Calorimetry' and 'Thermogravimetric Analysis' carried out on separate experiment (see figure 12 and 13).

In addition, the fact that the shifts in resonance frequency are negligible compared with the actual frequency ($\approx 0.03\%$), provides another indication that the compound is vibrating in the lattice rigid limit.

5.3. Problems encountered during the experiment

Firstly, it is important to mention that the equipment was only able to perform experiments in the temperature range of between 145 K and 366 K. This means that obtaining experimental results at lower and higher temperature were restricted, and analysis beyond the permitted range was not be possible.

Next, there are a few problems, which were encountered during the experiments. First, having performed the experiment on NaClO_3 compound, investigations on four further samples were carried out. Strong signals, which were thought to be the signal from the compounds, were detected in the first attempt to decide on the best samples to study. These signals, however, were not the signals from the compounds. This was discovered as the four signals were of identical frequency. In fact, this signal was thought to be a signal

from a radio station. To overcome these problems, the method of obtaining the NQR frequency was modified, i.e. two-pulse echo pulse was used in place of a single 90° pulse.

Secondly, failures to notice signals for three of the compounds were faced. These could be due to several factors: Firstly, it is probable that the compound was not totally crystallised, which could hinder signals being observed. Secondly, it could also be due to the fact that the relaxation times of the compound was so fast that observing the signal was difficult. Finally, since the experiment was performed in an NMR laboratory where the magnetic field is not zero, line broadening could have occurred and the signals could have become undetectable in the noise.

Finally, there was a problem to detect 'signals' as the temperature was lowered. This problem was thought to arise from a phase change in the compound. During the later part of the experiment, however, a 'hysteresis' effect was noticed, i.e. the measured value of the resonance frequency as the temperature is increased is not the same as the measured value of the resonance frequency as the temperature is decreased. The hysteresis effect was thought to be the reasons for the disappearance of the signals. Unfortunately, there was insufficient time to investigate the effect of hysteresis in the project.

5.4. Suggestions for future improvements

The present study can be improved in two ways. Firstly, by investigating the crystal structure of the compound in more depth and, secondly by studying the behaviour of ^{37}Cl isotopes of the compound. The structure of the compound could be investigated using X-ray diffraction and the result could be used to model the motions of the compound. The study of ^{37}Cl could determine the type of interaction that is occurring in the compound, and hence provide a more comprehensive review of the study.

6. Conclusion

^{35}Cl NQR frequency data shows the existence of a single phase with two resonance lines in 5-chloro-3-pyridinol. This indicates the presence of two chemically inequivalent positions for the chlorine nuclei in the unit cell. No broadening in the line width related to the re-orientation of ^{35}Cl in 5-chloro-3-pyridinol was observed, which indicates that the compound is vibrating in the lattice rigid limit. No evidence of phase change was observed in the results obtained. This is consistent with the data obtained from the temperature dependence of 'Differential Scanning Calorimetry' and 'Thermogravimetric Analysis'. Value of the activation energy of the motions of the compound was calculated to be $11.9 \pm 1.3 \text{ kJ mol}^{-1}$.

Acknowledgement

The author would like to thank all the people and copyright holders who gave permission to use facts and figures to help in the current project, the supervisor, Dr M.E. Smith, and the demonstrator, Dr I. Poplett, for their support and help in the projects. In addition, H.Tu is thanked for being a co-operative partner throughout the entire project.

References

- [1] S.C. Perez, R.L. Armstrong, A.H. Brunetti, (1993). 'A study of activated molecular motion in 2-nitrobenzene sulphonyl chloride by NQR', *Journal of Physics C: Condensed Matter*, **5**, pp. 4045-4054.
- [2] S.C. Perez, R.L. Armstrong, A.H. Brunetti, (1993). 'An NQR study of thermally activated molecular motion in 4-nitrobenzene sulphonyl chloride', *Journal of Physics C: Condensed Matter*, **5**, pp. 4055-4062.
- [3] T.P. Das, E.L. Hahn, (1958). 'Nuclear Quadrupole Resonance Spectroscopy', *Advances in Research and Applications, Supplement 1, Solid State Physics*, Academic Press Inc., Publishers New York. London.

- [4] H. Eckert, (1992). 'Structural characterisation of noncrystalline solids and glasses', *Progress in NMR spectroscopy*, **24**, pp.173-182.
- [5] R.K. Harris, *Nuclear Magnetic Resonance Spectroscopy*, Pitman, London, 1983.
- [6] M. Bloom and R.Norberg, (1954). 'Transient Nuclear Induction Signals Associated with Pure Quadrupole Interaction', *Physical Review*, **93**, pp. 638.
- [7] M. Bloom and R.Norberg, (1954). 'Slow beats in Nuclear Quadrupole Induction', *Physical Review*, **94**, pp. 1396.
- [8] C.J. Turner, (1975). 'Chlorine-35 Nuclear Quadrupole Resonance Spectra of Chlorodiazines', *Journal of the Chemical Society, Perkins*, **11**, pp. 1250-1252.